Properties of the quaternary half-metal-type Heusler alloy $Co_2Mn_{1-x}Fe_xSi$

Benjamin Balke, Gerhard H. Fecher, Hem C. Kandpal, and Claudia Felser*
Institut für Anorganische und Analytische Chemie, Johannes Gutenberg Universität, D-55099 Mainz, Germany

Keisuke Kobayashi, Eiji Ikenaga, Jung-Jin Kim, and Shigenori Ueda
Japan Synchrotron Radiation Research Institute (SPring-8/JASRI), Kouto 1-1-1, Mikaduki-cho, Sayou-gun, Hyogo, 679-5198, Japan
(Received 7 March 2006; revised manuscript received 20 July 2006; published 5 September 2006)

This paper reports on the bulk properties of the quaternary Heusler alloy $Co_2Mn_{1-x}Fe_xSi$ with the Fe concentration $x=0,1/2,1$. All samples, which were prepared by arc melting, exhibit $L2_1$ long-range order over the complete range of Fe concentration. The structural and magnetic properties of the $Co_2Mn_{1-x}Fe_xSi$ Heusler alloys were investigated by means of x-ray diffraction, high- and low-temperature magnetometry, Mössbauer spectroscopy, and differential scanning calorimetry. The electronic structure was explored by means of high-energy photoemission spectroscopy at about 8 keV photon energy. This ensures true bulk sensitivity of the measurements. The magnetization of the Fe-doped Heusler alloys is in agreement with the values of the magnetic moments expected for a Slater-Pauling-like behavior of half-metallic ferromagnets. The experimental findings are discussed on the basis of self-consistent calculations of the electronic and magnetic structure. To achieve good agreement with experiment, the calculations indicate that on-site electron-electron correlation must be taken into account, even at low Fe concentration. The present investigation focuses on searching for the quaternary compound where the half-metallic behavior is stable against outside influences. Overall, the results suggest that the best candidate may be found at an iron concentration of about 50%.

DOI: 10.1103/PhysRevB.74.104405 PACS number(s): 75.30.−m, 71.20.Be, 61.18.Fs

I. INTRODUCTION

Kübler *et al.*[1] recognized that the minority-spin state densities at the Fermi energy nearly vanish for Co_2MnAl and Co_2MnSn. The authors concluded that this should lead to peculiar transport properties in these Heusler compounds because only the majority density contributes. The so-called half-metallic ferromagnets have been proposed as ideal candidates for spin injection devices because they have been predicted to exhibit 100% spin polarization at the Fermi energy (ϵ_F).[2] From the applications point of view, a high Curie temperature for a half-metallic ferromagnet may be an important condition. For this reason, Heusler alloys with $L2_1$ structure have attracted great interest. Some of these alloys exhibit high Curie temperatures and, according to theory, should have a high spin polarization at the Fermi energy.[3–5] Calculations also show that antisite disorder will destroy the high spin polarization,[6] implying that precise control of the atomic structure of the Heusler alloys is required.

The Heusler alloy Co_2MnSi has attracted particular interest because it is predicted to have a large minority-spin band gap of 0.4 eV and, at 985 K, has one of the highest Curie temperatures among the known Heusler compounds.[7,8] Structural and magnetic properties of Co_2MnSi have been reported for films and single crystals.[9–14] In accordance with theoretical predictions, bulk Co_2MnSi has been stabilized in the $L2_1$ structure with a magnetization of $5\mu_B$ per formula unit. From tunneling magnetoresistance data with one electrode consisting of a Co_2MnSi film, Schmalhorst *et al.*[15,16] inferred a spin polarization of 61% at the barrier interface. Although the desired spin polarization of 100% was not reached, the experimental value of the spin polarization is larger than the maximum 55% effective spin polarization of a variety of 3*d* transition metal alloys in combination with Al_2O_3 barriers.[17] However, the spin polarization of photoelectrons emerging from single-crystalline Co_2MnSi films grown on GaAs by pulsed laser deposition indicate a quite low spin polarization at the Fermi level of only 12% at the free surface.[14] Wang *et al.*[13,14] assumed that partial chemical disorder was responsible for this discrepancy with the theoretical predictions.

Photoemission spectroscopy is the method of choice to study the occupied electronic structure of materials. Low kinetic energies result in a low electron mean free path, being only 5.2 Å at kinetic energies of 100 eV [all values calculated for Co_2FeSi using the Tanuma-Powell-Penn 2M equations[18]] and a depth of less than one cubic Heusler cell will contribute to the observed intensity. The situation becomes much better at high energies. In the hard x-ray region of about 8 keV one will reach a high bulk sensitivity with an escape depth being larger than 115 Å (corresponding to 20 cubic cells). High-energy photoemission (at about 15 keV excitation energy) was first performed[19] as early as 1989 using a ^{57}Co Mössbauer γ source for excitation, but with very low resolution only. Nowadays, high-energy excitation and analysis of the electrons become easily feasible due to the development of highly intense sources (insertion devices at synchrotron facilities) and multichannel electron detection. Thus, high-resolution–high-energy photoemission (HRHEPE) was recently introduced by several groups[20–25] as a bulk-sensitive probe of the electronic structure in complex materials. In the present work, HRHEPE at $h\nu \approx 8$ keV was used to study the density of states of $Co_2Mn_{1-x}Fe_xSi$ with $x=0,1/2,1$.

Recent investigations[26–29] of the electronic structure of Heusler compounds indicate that on-site correlation plays an important role in these compounds and may serve to destroy the half-metallic properties of Co_2MnSi. In addition, if on-site correlation is considered in electronic structure calcula-

tions Co_2FeSi becomes a half-metallic ferromagnet with a magnetic moment of $6\mu_B$.

The present investigation focuses on searching for a mixed compound in the series $Co_2Mn_{1-x}Fe_xSi$ where the half-metallic behavior is stable against the variation of on-site correlation and other outside influences.

II. COMPUTATIONAL DETAILS

The present paper reports, besides experiments, calculations of the electronic and magnetic properties of ordered Heusler compounds of the $Co_2(Mn_{1-x}Fe_x)Si$ type. The random alloys were treated as virtual crystals of the $Co_2Mn_{1-i/4}Fe_{i/4}Si$ type with $i=0,1,2,3,4$. Nonrational values of x as well as random disorder (for examples, see Refs. 30–32) will not be discussed here.

The self-consistent electronic structure calculations were carried out using the scalar-relativistic full potential linearized augmented plane wave (FLAPW) method as provided by WIEN2K.[33] In the parametrization of Perdew *et al.*[34] the exchange-correlation functional was taken within the generalized gradient approximation (GGA). A $20\times20\times20$ mesh was used for integration of cubic systems, resulting in 255 k points in the irreducible wedge of the Brillouin zone.

The properties of pure compounds containing Mn or Fe were calculated in $Fm\bar{3}m$ symmetry using the experimental lattice parameter ($a=10.658a_{0B}$, $a_{0B}=0.529177$ Å) determined by x-ray powder diffraction. Co atoms are placed on $8c$ Wyckoff positions, Mn or Fe on $4a$ and Si on $4b$.[51] All muffin tin radii were set as nearly touching spheres with $r_{MT}=2.3a_{0B}$. A structural optimization for the pure compounds showed that the calculated lattice parameter deviates from the experimental one only marginally.

The calculation of mixed random alloys is not straightforward in the FLAPW method as is used here. However, the substitution of some Mn atoms of the $L2_1$ structure by Fe leads in certain cases to ordered structures that can be easily used for the calculations. Those ordered, mixed compounds have the general formula sum $Co_8(Mn_{1-x}Fe_x)_4Si_4$ and have integer occupation of Mn and Fe if $x=i/4$ where $i=1,2,3$ (for more details see Ref. 32). To verify that ordered compounds could be used instead of random alloys, the full relativistic Korringa-Kohn-Rostocker (KKR) method with the coherent potential approximation (CPA) was employed.[35] The exchange-correlation functional was parametrized by using the plain GGA. No significant differences in the integrated properties, such as the density of states or the magnetic moments, were found between the methods.

For the case of Co_2FeSi, it has recently been demonstrated that the local spin density approximation (LSDA) or GGA schemes are not sufficient for describing the electronic structure correctly. Significant improvement was found, however, when the LDA+U method[26,29] was used and this computational scheme was used here as well. LDA+U, as described by Anisimov *et al.*,[36] adds an orbital-dependent electron-electron correlation, which is not included in the plain LSDA and GGA schemes. It should be mentioned that the +U was used in the FLAPW scheme with the GGA rather than the LSDA parametrization of the exchange-correlation functional. No significant differences were observed using either of these parametrizations.

III. EXPERIMENTAL DETAILS

$Co_2Mn_{1-x}Fe_xSi$ samples were prepared by arc melting of stoichiometric amounts of the constituents in an argon atmosphere at 10^{-4} mbar. Care was taken to avoid oxygen contamination. This was ensured by evaporating Ti inside the vacuum chamber before melting the compound as well as by additional purifying of the process gas. The polycrystalline ingots that were formed were then annealed in an evacuated quartz tube for 21 days. This procedure resulted in samples exhibiting the Heusler-type $L2_1$ structure, which was verified by x-ray powder diffraction (XRD) using excitation by Cu $K\alpha$ or Mo $K\alpha$ radiation.

Flat disks were cut from the ingots and polished for spectroscopic investigations of bulk samples. For powder investigations, the remainder was crushed by hand using a mortar. It should be noted that using a steel ball mill results in a strong perturbation of the crystalline structure.

X-ray photoemission [electron spectroscopy for chemical analysis (ESCA)] was used to verify the composition and to check the cleanliness of the samples. After removal of the native oxide from the polished surfaces by Ar^+ ion bombardment, no impurities were detected with ESCA. The samples were afterward capped *in situ* by a 2 nm layer of Au at room temperature to prevent oxidation of the samples during transport in air.

Magnetostructural investigations were carried out using Mössbauer spectroscopy in transmission geometry using a constant acceleration spectrometer. For excitation, a $^{57}Co(Rh)$ source with a linewidth of 0.105 mm/s (5 neV) was used. The spectra from powder samples were taken at 290 K.

The magnetic properties were investigated by a superconducting quantum interference device (SQUID, Quantum Design MPMS-XL-5) using nearly punctual pieces of approximately 5–10 mg of the sample. Differential scanning calorimetry (DSC) measurements (NETZCH, STA 429) were performed to detect phase transitions below the melting point. In particular, attempts were made to find the Curie temperature (T_C), but this turned out to be too high to be determined directly by the SQUID, which is limited to 775 K even in the high-temperature mode.

The electronic structure was explored by means of high-energy x-ray photoemission spectroscopy. The measurements were performed at the beamline BL47XU of the synchrotron SPring 8 (Hyogo, Japan). The photons are produced by means of a 140-pole undulator in vacuum and are further monochromatized by a double double-crystal monochromator. The first monochromator uses Si(111) crystals and the second a Si(111) channel-cut crystal with 444 reflections (for 8 keV x rays). The energy of the photoemitted electrons is analyzed using a Gammadata–Scienta R 4000 12 kV electron spectrometer. The ultimate resolution of the setup (monochromator plus analyzer at 50 eV pass energy using a 200 μm slit) is 83.5 meV at 7935.099 eV photon energy. For the experiments reported here, a photon energy of

TABLE I. $LDA+U$ parameter for $Co_2Mn_{1-x}Fe_xSi$. (All values are given in Ry.)

Element	Ref. 40 U_{dd}	Constrained LDA U	FLAPW U_{eff}	FPLMTO F^0	FPLMTO F^2	FPLMTO F^4
Co	0.194	0.3(1)	0.140	0.185	0.085	0.053
Fe	0.171	0.32	0.132	0.175	0.081	0.050
Mn	0.148	0.39	0.130	0.164	0.076	0.047

7939.15 eV has been employed. Under the present experimental conditions an overall resolution of 250 meV has been reached. All values concerning the resolution are determined from the Fermi edge of a Au sample. Due to the low cross section of the valence states from the investigated compounds, the spectra had to be taken with $E_{pass}=200$ eV and a 500 μm slit for a good signal-to-noise ratio. The polycrystalline samples have been fractured *in situ* before taking the spectra to remove the native oxide layer. Core-level spectra have been taken to check the cleanliness of the samples. No traces of impurities were found. The valence band spectra shown in Sec. IV E were collected over 2–4 h at about 100 mA electron current in the storage ring in the top-up mode. All measurements have been taken at a sample temperature of 20 K.

IV. RESULTS AND DISCUSSION

A. Electronic and magnetic structure

The electronic structure of the substitutional series $Co_2Mn_{1-i/4}Fe_{i/4}Si$ with $i=0,\ldots,4$ was calculated using the $LDA+U$ method. This method was used because it was found that plain GGA calculations are not sufficient to explain the magnetic moments in Co_2FeSi.[26] Using the impurity model of Anisimov and Gunnarsson[37] along with self-consistent calculations, the effective Coulomb-exchange parameter U_{eff} was determined for the pure compounds containing Mn and Fe. Details of the procedure and the implementation of the constrained LDA calculations in the FLAPW method are reported by Madsen and Novak.[38] The values found in the present work are $U_{Co}=0.30$ Ry and $U_{Mn}=0.39$ Ry for Co_2MnSi, and $U_{Co}=0.31$ Ry and $U_{Fe}=0.32$ Ry for Co_2FeSi.

Comparing the semiempirical values used in Ref. 29 to the values found here from the constrained LDA calculations, it is evident that the latter are too high to explain the magnetic moments. Additional calculations for the elemental $3d$ transition metals revealed that all values for U_{eff} found in the constrained LDA calculations are considerably too high to explain those metallic systems correctly. This is despite the fact that such calculations may result in reliable values for Mott insulators.[39]

For these reasons, the semiempirical values corresponding to 7.5% of the atomic values (see Ref. 29) will be used and discussed here for the case of the FLAPW calculations. These values ensure that the calculated magnetic moments agree with the measured values over the entire range of the Fe concentration (compare Sec. IV D). In particular, the values for U_{eff} were set to $U_{Co}=0.14$ Ry, $U_{Fe}=0.132$ Ry, and $U_{Mn}=0.13$ Ry, independent of the iron concentration. These values are closer to the values for the Coulomb interaction U_{dd} for d electrons in the elemental $3d$ transition metals reported by Bandyopadhyay and Sarma[40] even before the $LDA+U$ method itself was introduced.

The use of $U_{eff}=U-J$ suppresses multipole effects. That means, it neglects the nonspherical terms in the expansion of the Coulomb interaction. Additionally, full potential linearized muffin tin orbital (FPLMTO) calculations were performed to check for the influence of the nonspherical terms. In a different way, the LMTART 6.5 program provided by Savrasov[41] uses the Slater integrals $F^0,\ldots,F^4$ for the calculation of the on-site correlation with $U=F^0$ and $J=(F^2+F^4)/14$ (see also Refs. 36 and 37).

As in the FLAPW method, the use of the U values from the constrained LDA calculations leads also in the FPLMTO calculations to much too large values for the magnetic moments compared to the experimental findings. In the next step, only reduced values for F^0 were used. Following the arguments of Ref. 42, only F^0 should be affected by the screening in the solid state. However, the use of the atomic values for F^2 and F^4 as proposed in Ref. 42 still did not lead to satisfactory values for the magnetic moments. Finally, the reduction of all Slater integrals to 10% of their atomic values led to results compatible with the measured magnetic moments. Moreover, nearly identical results as in the FLAPW method were obtained concerning not only the magnetic moments but also the band structures. The slightly higher values resulting in the FPLMTO calculation are caused by the fact that these calculations used the U on top of the LDA exchange-correlation functional and not on top of the GGA parametrization. This behavior reveals that GGA includes some more correlation compared to the pure LDA. It is also observed within the FLAPW scheme.

The different values for U, U_{dd}, U_{eff}, and $F^0,\ldots,F^4$ are summarized in Table I. The values according to Ref. 40 were calculated for the d-state occupation as found from calculations using spherical potentials. The values for the FLAPW method are calculated from the Slater integrals reduced to 7.5% of the atomic values as calculated by Cowan's program[29,43] and the values for the FPLMTO method correspond to 10% of the atomic values. The use of these values leads to nearly identical results comparing FLAPW and FPLMTO methods.

In the following, only the results from the FLAPW calculations are discussed to allow for a better comparison with previous work. However, all results shown below are compatible and agree very well with those using $LDA+U$ in

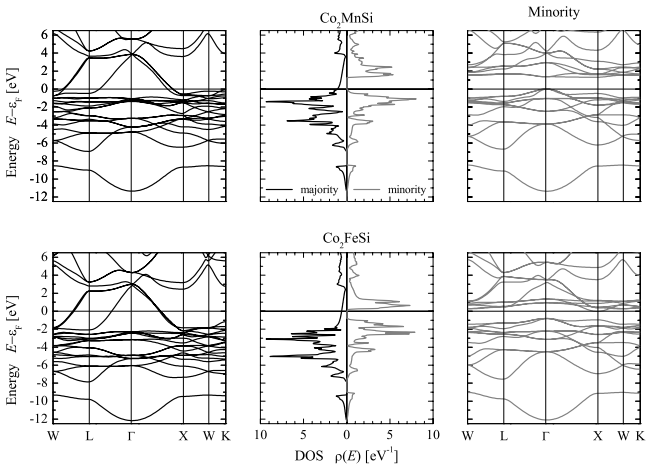

FIG. 1. Band structure and density of states of Co_2MnSi and Co_2FeSi.

FPLMTO calculations. Figure 1 shows the spin-resolved band structure and the total density of states for the pure compounds Co_2MnSi and Co_2FeSi as calculated within the framework of the LDA+U. In all cases, the band structures are very similar and the gap in the minority bands is clearly revealed.

When explaining the Heusler half-metallic ferromagnets using simple rigid-band-like or molecular-orbital-like models, it is expected that the additional d electron of the Fe compound fills the majority states while not affecting the minority states. As may be seen from Fig. 1, this is clearly a strong oversimplification. The additional electron must be absorbed in the strongly dispersing unoccupied d bands seen in the Mn compound just above ϵ_F. Comparing the majority density of states (DOS), it can be seen that the high-density d states at −1.4 eV (or −3.5 eV) in Co_2MnSi are shifted to approximately −3 eV (or −5 eV) in Co_2FeSi. Keeping the minority DOS fixed, this would imply an additional exchange splitting of about 1.6 eV, when compared to Co_2MnSi, between the majority and minority states in Co_2FeSi. This large and rather unphysical shift indicates that the rigid band model fails and that other alterations of the band structure must take place.

After inspecting the electronic structure in more detail, some particular changes are found. For example, the rather large shift of the occupied majority d states is compensated by a shift of the occupied minority d states, and this keeps the exchange splitting rather fixed. This then results in a shift and splitting of the occupied minority d states (seen at −1 eV in the Mn compound and at −1.7 or −2.3 eV in the Fe compound) as well as a shift of the unoccupied minority d states toward the Fermi energy. In addition, the splitting of the unoccupied minority d states just above the gap is reduced from 0.7 eV in Co_2MnSi to 0.4 eV in Co_2FeSi. The most striking effect, however, is the shift of the Fermi energy from the top of the minority valence band to the bottom of the minority conduction band. These particular positions of the minority gap with respect to the Fermi energy make both systems rather unstable with respect to their electronic and magnetic properties. Any small change of a physically relevant quantity may serve to destroy the half-metallic ferromagnet character by shifting the Fermi energy completely outside of the minority gap. As long as the shift is assumed to be small, the magnetic moment may still be similar to the one expected from Slater-Pauling behavior; even so, the minority gap is destroyed. For this reason, the magnetic moment may not provide evidence for a half-metallic state.

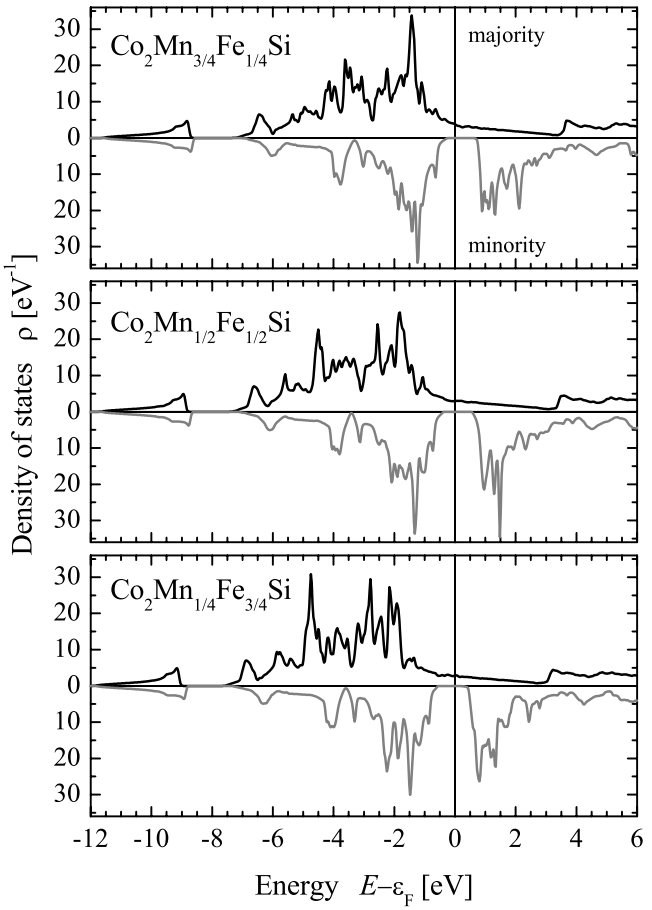

FIG. 2. Spin-resolved density of states of $Co_2Mn_{1-x}Fe_xSi$ for $x=1/4$, $1/2$, and $3/4$.

It is to be immediately expected that the situation improves in the mixed compounds containing both Mn and Fe. Figure 2 shows the spin-resolved total density of states for compounds with an intermediate Fe concentration ($x \neq 0, 1$). In all cases, the gap in the minority bands is kept.

The shift of the majority d states with low dispersion away from the Fermi energy is clearly visible in Fig. 2. The additional charge (with increasing Fe concentration x) fills the strongly dispersing d states in the majority channel. At the same time, the minority DOS is shifted with respect to the Fermi energy such that ϵ_F moves from the top of the minority valence bands at low x to the bottom of the minority conduction bands at high x. In general, it can be concluded that the additional electrons affect both majority and minority states.

Table II summarizes the results for the gap in the minority states as found from LDA+U calculations. The largest gap in the minority states is found for Co_2MnSi. The size of the gap decreases with increasing Fe content x, and at the same time, the position of the Fermi energy is moved from the top of the

TABLE II. Properties of the minority gap of ordered $Co_2Mn_{1-x}Fe_xSi$. Given are the extremal energies of the valence band maximum (VBM), the conduction band minimum (CBM), and the resulting gap (ΔE) in the minority states as found from LDA $+U$ calculations. The extremal energies are given with respect to ϵ_F. All energies are given in eV.

x	VBM	CBM	ΔE
0	0.003	1.307	1.3
1/4	−0.181	0.970	1.15
1/2	−0.386	0.495	0.88
3/4	−0.582	0.181	0.86
1	−0.810	−0.028	0.78

valence band to the bottom of the conduction band. It is also seen that the compounds with $x=0$ and 1 are on the borderline of half-metallic ferromagnetism, as the Fermi energy just touches the top of the valence band or the bottom of the conduction band. In both cases, a slight change of U_{eff} in the calculation is able to shift ϵ_F outside of the gap in the minority states.

For intermediate Fe concentration, the Fermi energy falls close to the middle of the gap in the minority states (see also Fig. 2). This situation makes the magnetic and electronic properties of the compound very stable against external influences that will not be able to change the number of minority electrons. This applies both to the parameters in the theoretical calculations as well as to the actual experimental situation. From this observation it can be concluded that $Co_2Mn_{1/2}Fe_{1/2}Si$ exhibits a very stable half-metallic character in this series of compounds, as well as those with a concentration close to $x=0.5$.

If the Heusler alloys are half-metallic ferromagnets, then they will show a Slater-Pauling behavior for the magnetization, meaning that the saturation magnetization scales with the number of valence electrons.[3,5,44] The magnetic moment per unit cell (in multiples of the Bohr magneton μ_B) is given by

$$m = N_V - 24, \tag{1}$$

with N_V denoting the accumulated number of valence electrons in the unit cell. For Co_2MnSi there is a total of $2\times 9+7+4=29$ valence electrons in the unit cell and accordingly 30 for Co_2FeSi; for this reason the magnetic moment is expected to vary linearly from $5\mu_B$ to $6\mu_B$ with increasing iron concentration in $Co_2Mn_{1-x}Fe_xSi$.

The results found from the LDA$+U$ calculations for the magnetic moments are summarized in Table III and compared to pure GGA calculations without the inclusion of the U type correlation. It is evident from Table III that the GGA-derived values do not follow the Slater-Pauling curve (with the exception of Co_2MnSi), whereas the values from the LDA$+U$ follow the curve closely. These results again indicate the loss of the minority gap—and thus the loss of half metallicity—if the on-site correlation is not included.

TABLE III. Total magnetic moments of ordered $Co_2Mn_{1-x}Fe_xSi$. All moments were calculated for the given supercells. Their values are in μ_B and assume four atoms in the unit cell for easier comparison.

Compound	x	GGA	LDA$+U$
Co_2MnSi	0	5.00	5.00
$Co_8Mn_3FeSi_4$	1/4	5.21	5.25
$Co_4MnFeSi_2$	1/2	5.44	5.50
$Co_8MnFe_3Si_4$	3/4	5.55	5.75
Co_2FeSi	1	5.56	6.00

B. Structural properties

Structural characterization has been performed with x-ray diffraction of powders as the standard method. Due to the small differences in the scattering factors between the 3d metals Mn, Fe, and Co, structural information, other than a simple confirmation of a single cubic phase, can only be gained by measuring the comparatively small [5% of the (220) peak] (111) and (200) superstructure peaks that are typical for the face centered cubic (fcc) lattice. The simulated powder diffraction pattern of Co_2MnSi MnSi shows the decisive (111) and (200) peaks for the defect-free structure. Both of these superlattice peaks vanish for a random occupation of all lattice sites (4a, 4b, and 8c) resulting in the $A2$ structure. In the case of random occupation of 4a and 4b sites by Mn, Fe, and Si, only the (200) superlattice peak of the $B2$ structure type would be seen, while the (111) peak would vanish.

Such types of disorder would close the gap in the minority DOS so that the material would no longer be a half-metallic ferromagnet.[28,32] However, the magnetic moments may still follow a Slater-Pauling-like behavior. The half-metallic character is also destroyed when only one of the Co atoms is exchanged by Mn or Fe (X structure[45] with symmetry $F\bar{4}3m$). This type of disorder shows up as a (111) superlattice peak with higher intensity than the (200) peak.

As expected for the defect-free structure, the experimental data show both the (111) and (200) peaks with equal intensity for all Fe concentrations, indicating the presence of a long-range fcc structure for all samples (see Fig. 3). Within the uncertainty of the experiment, the lattice parameter of 5.64 Å remains nearly independent of the Fe concentration.

Because the scattering factors of all three transition metals are very similar, x-ray diffraction cannot easily discern a disorder when the Mn and Fe are partially exchanged with Co atoms on both 8a positions ($D0_3$-like disorder). Because both have the same $Fm\bar{3}m$ symmetry, this leads to nearly identical diffraction patterns when going from the $L2_1$ to the $D0_3$ structure. As will be shown in the next section, this type of disorder can be ruled out by means of Mössbauer spectroscopy.

C. Magnetostructural properties

^{57}Fe Mössbauer spectroscopy was performed to investigate the magnetostructural properties. The transmission spec-

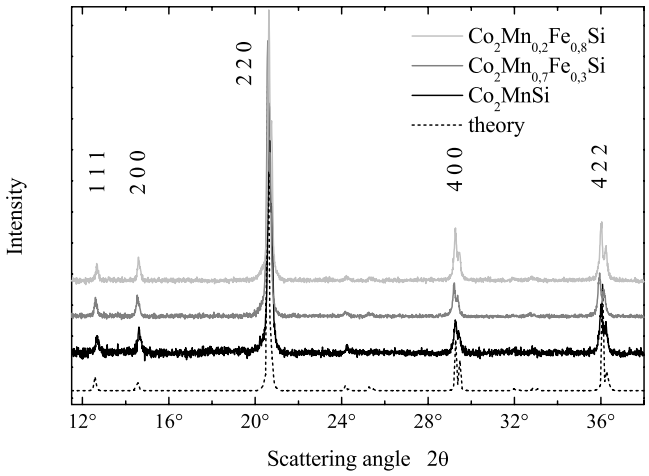

FIG. 3. XRD spectra for Co_2MnSi and $Co_2Mn_{0.8}Fe_{0.2}Si$.The spectra were excited by Mo K_α radiation.

trum of $Co_2Mn_{0.5}Fe_{0.5}Si$ is shown in Fig. 4. Starting from 10%, the spectra for the complete range of Fe concentrations x are all similar and therefore not shown here. The observed sextetlike pattern is typical for a magnetically ordered system. The pattern is typical for the cubic symmetry and no asymmetric shift of the lines from a noncubic quadrupole interaction is observed.

The spectrum shown in Fig. 4 for 50% Fe is dominated by an intense sextet. With Fe occupying the 4*a* sites with cubic symmetry (O_h), this sextet indicates the high order of the sample. In addition to the sextet, a much weaker line at the center of the spectrum is visible. Depending upon the composition it can be explained as a singlet or doublet. Its contribution to the overall intensity of the spectrum is approximately 3.5% at $x=0.5$. The origin of the singlet or doublet may be antisite disorder leading to a small fraction of paramagnetic Fe atoms. The splitting of the paramagnetic line into a doublet is due to dynamic effects and, among others reasons, usually depends upon the size of the powder grains.

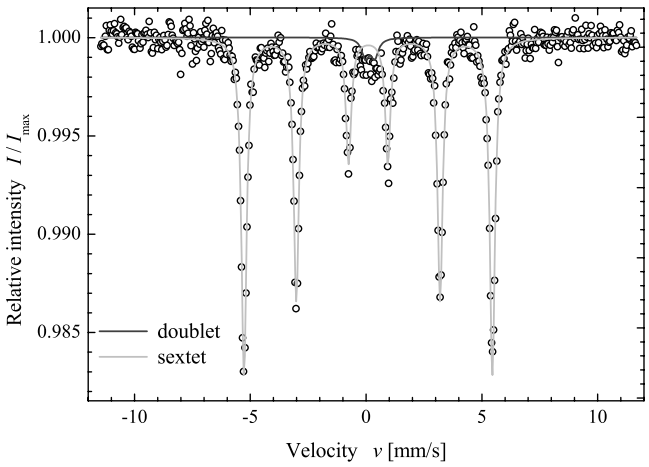

FIG. 4. ^{57}Fe Mössbauer spectrum of $Co_2Mn_{0.5}Fe_{0.5}Si$. The spectrum was taken at 290 K and excited by a $^{57}Co(Rh)$ source. Solid lines are results of a fit to determine the sextet and doublet contributions and to evaluate the hyperfine field.

TABLE IV. Mössbauer data for iron in $Co_2Mn_{1-x}Fe_xSi$. Given are the measured and calculated values of the hyperfine field (H_{hff}) and the measured isomer shift (IS) for increasing Fe concentration x.

	H_{hff} (10^6 A/m)		
x	Experiment	Calculation	IS (neV)
0.1	25.937		3.61
0.2	26.214		3.77
0.25		26.534	
0.4	26.412		4.18
0.5	26.466	26.629	4.34
0.6	26.417		4.75
0.7	26.259		4.90
0.75		26.962	
0.8	25.915		5.33
0.9	25.480		5.77
1	24.997	27.013	6.21

The slight disorder arises most likely from surface regions of the sample that are destroyed when the sample is crushed to powder. A partial contamination of the relatively large surface area of the powder with oxygen can also not be excluded. The relative contribution of the doublet decreases exponentially from 9% in low-Fe-substituted $Co_2Mn_{0.9}Fe_{0.1}Si$ to 1.8% in pure Co_2FeSi. As was also suggested by the photoabsorption and ESCA measurements, this may indicate a larger probability for oxidation in the Mn-rich part of the series.

The linewidth of the sextet is approximately 0.14 ± 0.01 mm/s (corresponding to 6.7 neV) on average over the complete series of compositions. A markedly higher linewidth of ≈ 0.19 mm/s was found for the alloy with $x=0.7$. This indicates a higher disorder in that sample and may also explain the slightly higher magnetic moment (compare Fig. 8 in Sec. IV D). The isomer shift increases linearly from 0.075 mm/s (3.6 neV) to 0.129 mm/s (6.2 neV) with increasing x, indicating the change in the environment of the Fe atoms, which appears here in the second-nearest-neighbor shell where the next Fe or Mn atoms are located. Despite this increase, the values suggest an Fe^{3+}-like character of the iron atoms in $Co_2Mn_{1-x}Fe_xSi$. The increase points to a slight decrease of the valence electron concentration close to the iron atoms. Table IV summarizes the values for the isomer shift and the hyperfine field (H_{hff}) as functions of the iron concentration.

The hyperfine field at the Fe sites amounts to 26.5×10^6 A/m in $Co_2Mn_{0.5}Fe_{0.5}Si$. This is the maximum value observed in the complete series with varying Fe concentration x. Overall, the hyperfine field varies nonlinearly from 25.9×10^6 A/m at $x=0.1$ to 25×10^6 A/m at $x=1$ (see also Ref. 52). For low iron concentration, it increases with x and decreases from $x=0.5$ to $x=1$. It should be noted that the Mössbauer spectra taken at 85 K from Co_2FeSi exhibited a considerably higher value (26.3×10^6 A/m) without additional singlet or doublet contributions. Therefore, thermally

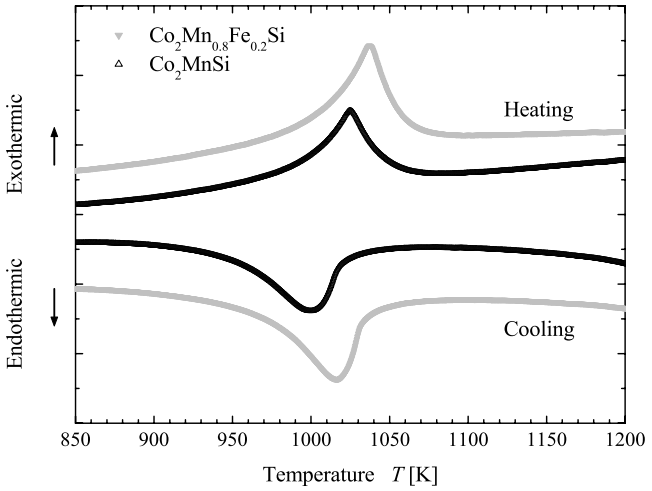

FIG. 5. DSC results for Co_2MnSi and $Co_2Mn_{0.8}Fe_{0.2}Si$.

activated fluctuations or disorder cannot be excluded here. The values of the hyperfine field at the Fe atoms are comparable to those found by Niculescu *et al.*[46,47] using spin-echo nuclear magnetic resonance (NMR). For $Co_{3-x}Fe_xSi$, these authors reported approximately 26.9×10^6 A/m for iron on 4*a* sites. The values for partial occupancy of 8*c* sites expected from NMR ($\approx16\times10^6$ A/m) for Co_2FeSi are considerably smaller.[47] This is in agreement with calculations for Co and Fe on interchanged sites ($\approx17\times10^6$ A/m). Therefore, a $D0_3$-type disorder can be excluded. The calculated hyperfine fields are, however, nearly independent of the Fe concentration. They decrease linearly with x by -0.7×10^6 A/m from 27.01×10^6 A/m for Co_2FeSi. A maximum in the $H_{hff}(x)$ dependence at $x=1/2$ could not be verified. It was found neither for the ordered compounds using the FLAPW method with the LDA+U (see Table IV), nor for random alloys calculated using a KKR CPA scheme in the GGA approximation.[53]

Differential scanning calorimetry was used to find the high-temperature phase transitions in the substitutional series. Figure 5 shows a typical result from DSC, which was used to investigate the expected phase transitions. The figure displays the change of the DSC signal as a function of the temperature using nominal heating and cooling rates of 20 K/min. A strong signal arising from a phase transition is easily detected at about 1000–1050 K during both heating and cooling. The shift of the maxima is mainly due to an intrinsic hysteresis effect of the method and depends on the temperature rates and the actual amount of material. The length of the error bars in Fig. 6 corresponds to this hysteresis.

A series of DSC measurements was performed with different scanning rates for heating and cooling, but it was not possible to distinguish the magnetic transition temperature because it was too close to the structural transition temperature of the $L2_1$ to the $B2$ phase $T_t^{B2\leftrightarrow L2_1}$. To overcome the problem of nearby phase transitions of a different kind, it would be necessary to obtain high-temperature magnetization curves such as those that Kobayashi *et al.*[48] obtained in their examination of the series $Co_2Cr_{1-x}Fe_xGa$, or the difference in the transition temperatures should be more than 100 K.

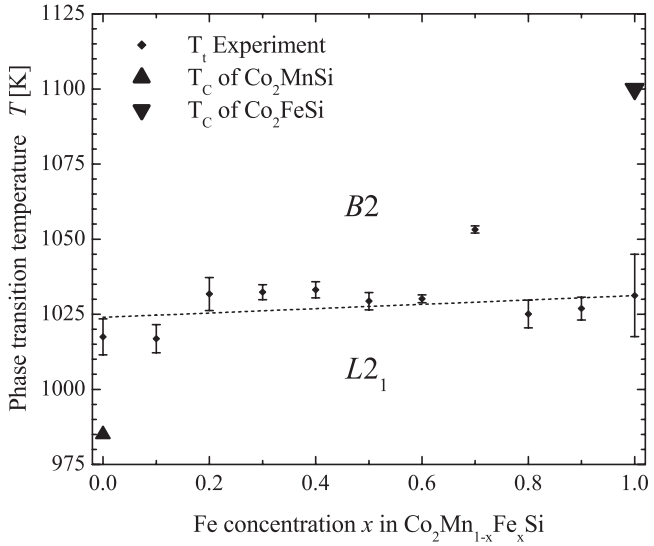

FIG. 6. Phase transitions in $Co_2Mn_{1-x}Fe_xSi$. The straight line is the result of a linear fit of $T_t(x)$ as function of the Fe concentration. The given Curie temperatures are taken from Refs. 49 and 26 for Co_2MnSi and Co_2FeSi, respectively.

Figure 6 displays the temperature dependence of the $L2_1\leftrightarrow B2$ phase transition. It is nearly constant, increasing slightly, as the Fe content increases, from ≈1024 K for Co_2MnSi to ≈1031 K for Co_2FeSi. It is seen that the Curie temperatures of the end members of the substitutional series are slightly below or above the structural phase transition for the compound containing Mn or Fe, respectively. The Curie temperature is expected to increase with increasing x from $T_C(0)=985$ K (Ref. 49) to $T_C(1)=1100$ K,[26] while in $Co_2Mn_{1-x}Fe_xSi$ $T_t^{B2\leftrightarrow L2_1}$ hardly varies with increasing x, being around 1027 K for $x=0.5$. It is therefore impossible here to unambiguously determine T_C by using the DSC technique, because of the relative weakness of the magnetic transition compared to the structural transition and the overlap of those two transitions in the DSC spectra. It is interesting to note that the Curie temperature of the compounds with high Fe concentration appears to be above the order-disorder phase transition.

D. Magnetic properties

The Co_2-based Heusler alloys that are half-metallic ferromagnets show a Slater-Pauling-like behavior for the magnetization (see Sec. IV A). The saturation magnetization scales with the number of valence electrons[5] and the magnetic moment per unit cell is given by Eq. (1). A magnetic moment of

$$m(x)=(5+x)\mu_B \tag{2}$$

is expected for $Co_2Mn_{1-x}Fe_xSi$.

Low-temperature magnetometry was performed by means of the SQUID to check the calculated saturation moment. Selected results are shown in Fig. 7. The increase of the saturation moment with the iron concentration is clearly visible. In addition, it is found that all $Co_2Mn_{1-x}Fe_xSi$ samples are soft magnetic with a small remanence and a small coer-

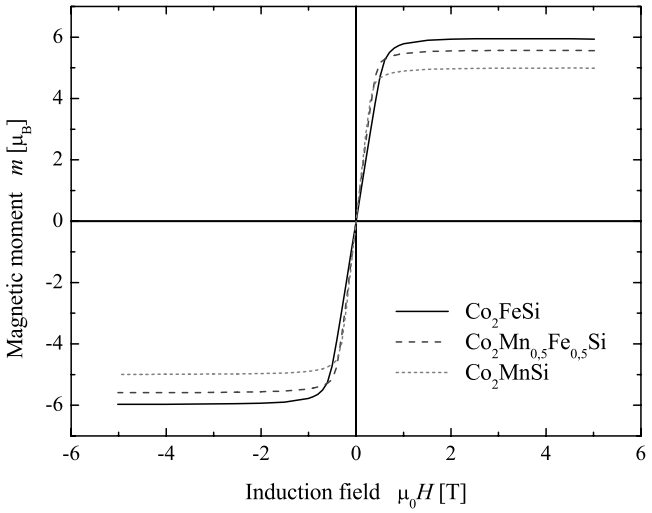

FIG. 7. Magnetization of $Co_2Mn_{1-x}Fe_xSi$. Displayed are the hysteresis curves for $x=0,0.5,1$ taken at $T=5$ K.

cive field. Results for the element-specific magnetic moments from x-ray magnetic circular dichroism are reported elsewhere.[50]

The total magnetic moments, measured at 5 K and in saturation, are $(4.97\pm0.05)\mu_B$ and $(5.97\pm0.05)\mu_B$ for the pure compounds Co_2MnSi and Co_2FeSi, respectively. The latter is in perfect agreement with the recent investigation reported in Refs. 26 and 27. Figure 8 displays the dependence of the saturation moment as a function of the Fe concentration x. The series shows a nearly linear increase of m with increasing Fe concentration that closely fits the values expected from a Slater-Pauling-like behavior.

Comparing the experimental results to the theoretical values as given in Table III, it is evident that they closely agree with those from the LDA+U calculations. The agreement of the GGA result for Co_2MnSi may thus be seen as due to chance. The comparison also substantiates the use of correlation energies of about 0.135 Ry, as these can be used to predict the magnetic moment correctly over the entire range of Fe concentration x.

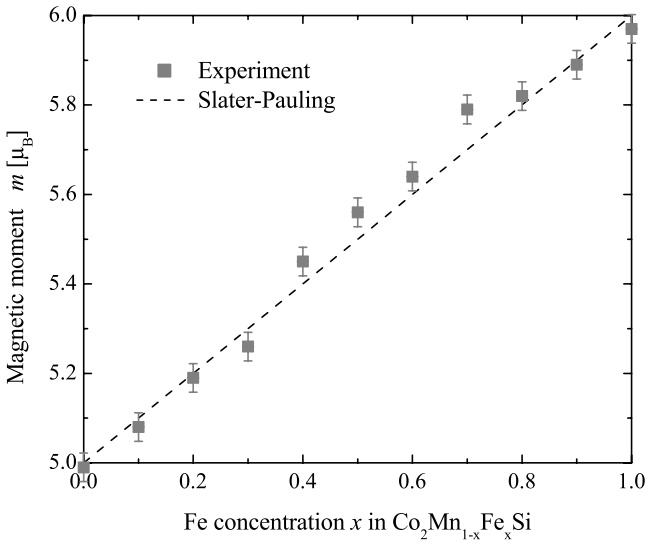

FIG. 8. Concentration dependence of the magnetic moment in $Co_2Mn_{1-x}Fe_xSi$. All measurements were performed at $T=5$ K.

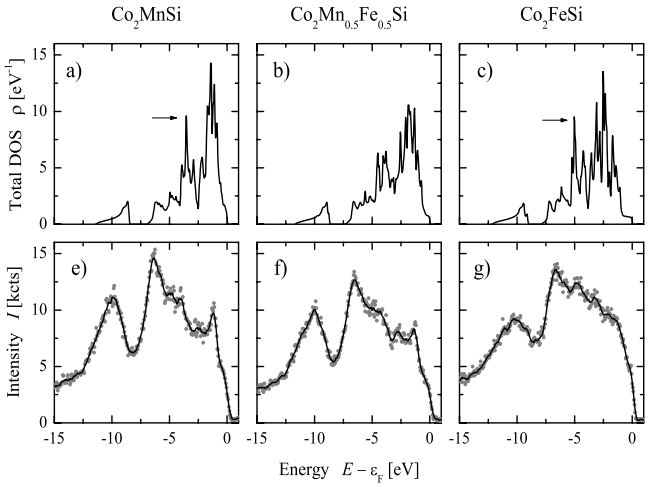

FIG. 9. Valence density of $Co_2Mn_{1-x}Fe_xSi$ ($x=0,1/2,1$). The calculated total density of states (a), (b), (c) has been convoluted with a Fermi-Dirac distribution using $T=20$ K. The photoelectron spectra (e), (f), (g) have been excited by $h\nu=7.939$ keV.

E. Electronic properties

The results from high-energy photoemission are shown in Fig. 9 and compared to the total density of states calculated for $Co_2Mn_{1-x}Fe_xSi$ with $x=0,1/2,1$. The calculated total DOS is the sum of the spin-resolved majority and minority DOSs shown in Figs. 1 and 2 and convoluted with a Fermi-Dirac distribution using $T=20$ K.

The spectra of all three compounds reveal clearly the low-lying s states at about -11 to -9 eV below the Fermi energy, in good agreement with the calculated DOS. These low-lying bands are separated from the high-lying d states by the Heusler-typical hybridization gap which is clearly resolved in the spectra as well as the calculated DOS. The size of this gap amounts typically to $\Delta E\approx 2$ eV in Si-containing compounds.

Obviously, the emission from the low-lying s states is greatly enhanced compared to the emission from the d states. This can be explained by a different behavior of the cross sections of the s, p, and d states with increasing kinetic energy as was recently demonstrated by Panaccione *et al.* for the case of the silver valence band.[24] In particular, the cross section for d states decreases faster with increasing photon energy than the one of the s states. This behavior influences also the onset of the d bands at about -7 eV. Just at the bottom of those d bands, they are hybridized with s,p-like states, leading to a high intensity in this energy region.

The structure of the spectra in the range of the d states agrees with the structures observed in the total DOS. However, one has to account for lifetime broadening and the experimental resolution if comparing that energy range. The lowest flatband of the majority band structure (see Fig. 1), accompanying the localized moment at the Y sites, results in a sharp peak in the DOS at about -3.5 and -5 eV for Mn and

Fe, respectively [marked by arrows in Figs. 9(a) and 9(c)]. These peaks are shifted away from ϵ_F by the electron-electron correlation in the LDA+U calculation and would appear without U closer to the Fermi energy. Their energetic position corresponds to structures revealed in the measured spectra; thus they are a good proof for the use of the LDA+U scheme.

Most interesting is the behavior of the calculated DOS and the measured spectra close to ϵ_F as this might give information about the gap in the minority states. The majority band structure contributes only a few states to the density at ϵ_F emerging from strongly dispersing bands. This region of low density is enclosed by a high density of states arising from flatbands at the upper and lower limits of the minority band gap. The onset of the minority valence band is clearly seen in the total DOS as well as the low majority density at the Fermi energy. The same behavior is observed in the measured valence band spectra. From the spectra, it can be estimated that the Fermi energy is in all three cases about 0.5 eV above the minority valence band. This gives strong evidence that all compounds of the $Co_2Mn_{1-x}Fe_xSi$ series exhibit really half-metallic ferromagnetism.

The values for U_{eff} used in Sec. IV A are the borderline cases for the half-metallic ferromagnetism over the complete series $Co_2Mn_{1-x}Fe_xSi$. They were used as independent of the Fe concentration, as was suggested for Co from the constrained LDA calculations. However, the valence band spectra shown in Fig. 9 indicate that the Fermi energy of both end members may fall inside the minority gap rather than being located at the edges of the minority gap. This situation may be simulated by a variation of U. A comparison to the U dependence of the minority gap shown in Ref. 29 suggests smaller effective Coulomb exchange parameters for the Mn-rich part and larger ones for the Fe-rich part of the series. This might also explain the nonlinearity reported in Sec. IV D for the hyperfine field. A variation of those parameters for all contributing 3d constituents in the calculations was omitted here because it would not bring more insight into the nature of the problem, at present.

Overall, the measured photoelectron spectra agree well with the calculated density of states and principally verify the use of the LDA+U scheme. In particular, the shape of the spectra close to ϵ_F can be explained by the occurrence of a gap in the minority states and thus points indirectly to the half-metallic state of all three compounds investigated here by photoemission. For clarity about the gap, spin-resolved photoemission spectroscopy at high energies would be highly desirable. However, this will require another step of improvement of the instrumentation necessary, for both photon sources as well as electron energy and spin analyzers, as the spin detection will need a factor of at least three to four orders of magnitude more intensity for a single energy channel at the same resolution as used here for the intensity spectra.

V. SUMMARY AND CONCLUSION

The substitutional series of the quaternary Heusler compound $Co_2Mn_{1-x}Fe_xSi$ was synthesized and investigated both experimentally and theoretically.

The results found from the LDA+U calculations for the magnetic moments $m(x)$ closely follow the Slater-Pauling curve. The shift of the minority gap with respect to the Fermi energy, from the top of the minority valence band for Co_2MnSi to the bottom of the minority conduction band for Co_2FeSi, makes both systems rather unstable with respect to their electronic and magnetic properties. The calculated band structures suggest that the most stable compound in a half-metallic state will occur at an intermediate Fe concentration. These theoretical findings are supported by the experiments.

All samples of the substitutional series exhibit an $L2_1$ order that is independent of the Fe concentration x. The observed structural order-disorder phase transition from $L2_1$ to $B2$ is nearly independent of x and occurs at about 1030 K. Mössbauer measurements show only a negligible paramagnetic contribution confirming the high degree of order over the whole substitutional series. In agreement with the expectation from the Slater-Pauling curve, the magnetic moment increases linearly with x from $5\mu_B$ to $6\mu_B$. True bulk-sensitive, high-energy photoemission bears out the inclusion of electron-electron correlation in the calculation of the electronic structure and gave indirect evidence for the gap in the minority states. Both valence band spectra and hyperfine fields indicate an increase of the effective Coulomb-exchange parameters with increasing Fe concentration.

From both the experimental and computational results it is concluded that a compound with an intermediate Fe concentration of about 50% should be most stable and best suited for spintronic applications.

ACKNOWLEDGMENTS

The authors are grateful for the support by G. Schönhense and thank J. Thoenies and A. Lotz for help with the calculation of U_{eff} as well as V. Jung, V. Ksenofontov, and S. Reimann (Mainz) for performing the Mössbauer experiments, and Y. Takeda (Spring-8, Japan) for help during the beam time. The synchrotron radiation experiments were performed at the beamline BL47XU of SPring-8 with the approval of the Japan Synchrotron Radiation Research Institute (JASRI) (Proposal No. 2006A1476). This work was partially supported by a Grant-in-Aid for Scientific Research (A) (No. 15206006), and also partially supported by a Nanotechnology Support Project, of The Ministry of Education, Culture, Sports, Science and Technology of Japan. Financial support by the Deutsch Forschungsgemeinschaft (Projects No. TP1 and No. TP7 in research group FG 559) is gratefully acknowledged.

*Electronic address: fecher@uni-mainz.de

[1] J. Kübler, A. R. Williams, and C. B. Sommers, Phys. Rev. B **28**, 1745 (1983).
[2] R. A. de Groot, F. M. Müller, P. G. van Engen, and K. H. J. Buschow, Phys. Rev. Lett. **50**, 2024 (1983).
[3] I. Galanakis, P. H. Dederichs, and N. Papanikolaou, Phys. Rev. B **66**, 174429 (2002).
[4] S. Picozzi, A. Continenza, and A. J. Freeman, Phys. Rev. B **66**, 094421 (2002).
[5] G. H. Fecher, H. C. Kandpal, S. Wurmehl, and C. Felser, J. Appl. Phys. **99**, 08J106 (2006).
[6] S. Picozzi, A. Continenza, and A. J. Freeman, Phys. Rev. B **69**, 094423 (2004).
[7] S. Fuji, S. Sugimura, S. Ishida, and S. Asano, J. Phys.: Condens. Matter **2**, 8583 (1990).
[8] P. J. Brown, K.-U. Neumann, P. J. Webster, and K. R. A. Ziebeck, J. Phys.: Condens. Matter **12**, 1827 (2000).
[9] M. P. Raphael, B. Ravel, Q. Huang, M. A. Willard, S. F. Cheng, B. N. Das, R. M. Stroud, K. M. Bussmann, J. H. Claassen, and V. G. Harris, Phys. Rev. B **66**, 104429 (2002).
[10] U. Geiersbach, A. Bergmann, and K. Westerholt, J. Magn. Magn. Mater. **240**, 546 (2002).
[11] S. Kämmerer, S. Heitmann, D. Meyners, D. Sudfeld, A. Thomas, A. Hütten, and G. Reiss, J. Appl. Phys. **93**, 7945 (2003).
[12] L. J. Singh, Z. H. Barber, Y. Miyoshi, Y. Bugoslavsky, W. R. Branford, and L. F. Cohen, Appl. Phys. Lett. **84**, 2367 (2004).
[13] W. H. Wang, M. Przybylski, W. Kuch, L. I. Chelaru, J. Wang, Y. F. Lu, J. Barthel, H. L. Meyerheim, and J. Kirschner, Phys. Rev. B **71**, 144416 (2005).
[14] W. H. Wang, M. Przybylskia, W. Kuch, L. I. Chelaru, J. Wang, Y. F. Lu, J. Barthel, and J. Kirschner, J. Magn. Magn. Mater. **286**, 336 (2005).
[15] J. Schmalhorst, S. Kammerer, M. Sacher, G. Reiss, A. Hütten, and A. Scholl, Phys. Rev. B **70**, 024426 (2004).
[16] J. Schmalhorst, S. Kammerer, G. Reiss, and A. Hütten, Appl. Phys. Lett. **86**, 052501 (2005).
[17] P. LeClair, H. J. M. Swagten, J. T. Kohlhepp, and W. J. M. de Jonge, Appl. Phys. Lett. **76**, 3783 (2000).
[18] S. Tanuma, C. J. Powell, and D. R. Penn, Surf. Interface Anal. **21**, 165 (1993).
[19] W. Meisel, Hyperfine Interact. **45**, 73 (1989).
[20] K. Kobayashi *et al.*, Appl. Phys. Lett. **83**, 1005 (2003).
[21] A. Sekiyama and S. Suga, J. Electron Spectrosc. Relat. Phenom. **137-140**, 681 (2004).
[22] S. Thiess, C. Kunz, B. C. C. Cowie, T.-L. Lee, M. Reniera, and J. Zegenhagen, Solid State Commun. **132**, 589 (2004).
[23] K. Kobayashi, Nucl. Instrum. Methods Phys. Res. A **547**, 98 (2005).
[24] G. Panaccione *et al.*, J. Phys.: Condens. Matter **17**, 2671 (2005).
[25] P. Torelli *et al.*, Rev. Sci. Instrum. **76**, 023909 (2005).
[26] S. Wurmehl, G. H. Fecher, H. C. Kandpal, V. Ksenofontov, C. Felser, H.-J. Lin, and J. Morais, Phys. Rev. B **72**, 184434 (2005).
[27] S. Wurmehl, G. H. Fecher, H. C. Kandpal, V. Ksenofontov, C. Felser, and H.-J. Lin, Appl. Phys. Lett. **88**, 032503 (2006).
[28] S. Wurmehl *et al.*, J. Phys. D **39**, 803 (2006).
[29] H. C. Kandpal, G. H. Fecher, C. Felser, and G. Schönhense, Phys. Rev. B **73**, 094422 (2006).
[30] Y. Miura, K. Nagao, and M. Shirai, Phys. Rev. B **69**, 144413 (2004).
[31] K. Kobayashi, R. Y. Umetsu, R. Kainuma, K. Ishida, T. Oyamada, A. Fujita, and K. Fukamichi, Appl. Phys. Lett. **85**, 4684 (2004).
[32] G. H. Fecher, H. C. Kandpal, S. Wurmehl, J. Morais, H.-J. Lin, H.-J. Elmers, G. Schönhense, and C. Felser, J. Phys.: Condens. Matter **17**, 7237 (2005).
[33] P. Blaha, K. Schwarz, G. K. H. Madsen, D. Kvasnicka, and J. Luitz, computer code WIEN2K (Karlheinz Schwarz, Techn. Universitaet Wien, Wien, Austria, 2001).
[34] J. P. Perdew, J. A. Chevary, S. H. Vosko, K. A. Jackson, M. R. Pederson, D. J. Singh, and C. Fiolhais, Phys. Rev. B **46**, 6671 (1992).
[35] H. Ebert, in *Electronic Structure and Physical Properties of Solids: The Use of the LMTO Method*, edited by H. Dreysee, Lecture Notes in Physics Vol. 535 (Springer-Verlag, Berlin, 1999), pp. 191–246.
[36] V. I. Anisimov, F. Aryasetiawan, and A. I. Lichtenstein, J. Phys.: Condens. Matter **9**, 767 (1997).
[37] V. I. Anisimov and O. Gunnarsson, Phys. Rev. B **43**, 7570 (1991).
[38] G. K. H. Madsen and P. Novak, Europhys. Lett. **69**, 777 (2005).
[39] V. I. Anisimov, J. Zaanen, and O. K. Andersen, Phys. Rev. B **44**, 943 (1991).
[40] T. Bandyopadhyay and D. D. Sarma, Phys. Rev. B **39**, 3517 (1989).
[41] S. Y. Savrasov, Phys. Rev. B **54**, 16470 (1996).
[42] V. I. Anisimov, I. V. Solovyev, M. A. Korotin, M. T. Czyzyk, and G. A. Sawatzky, Phys. Rev. B **48**, 16929 (1993).
[43] R. D. Cowan, *The Theory of Atomic Structure and Spectra* (University of California Press, Berkeley, 1981).
[44] D. Jung, H. J. Koo, and M. H. Whangbo, J. Mol. Struct.: THEOCHEM **527**, 113 (2000).
[45] G. E. Bacon and J. S. Plant, J. Phys. F: Met. Phys. **1**, 524 (1971).
[46] V. Niculescu, T. J. Burch, K. Rai, and J. I. Budnick, J. Magn. Magn. Mater. **5**, 60 (1977).
[47] V. Niculescu, J. I. Budnick, W. A. Hines, K. Raj, S. Pickart, and S. Skalski, Phys. Rev. B **19**, 452 (1979).
[48] K. Kobayashi, R. Y. Umetsu, A. Fujita, K. Oikawa, R. Kainuma, K. Fukamichi, and K. Ishida, J. Alloys Compd. **399**, 60 (2005).
[49] P. J. Webster, J. Phys. Chem. Solids **32**, 1221 (1971).
[50] M. Kallmayer, H. J. Elmers, B. Balke, S. Wurmehl, F. Emmerling, G. H. Fecher, and C. Felser, J. Phys. D **39**, 786 (2006).
[51] Note that 4*a* and 4*b* positions are equivalent; for clarity we assume that Si is always on 4*b*.
[52] Note that the Mössauer data reported in Ref. 26 were taken at lower temperature (85 K).
[53] Note that these calculations need at present a rather unphysical enlargement of the lattice parameter in order to explain the magnetic moments and position of the minority gap correctly.